Slow magnetic relaxation influenced by symmetry change from ideal C_i to D_{3d} in cobalt(II)-based single-ion magnets

Lei Chen,[a] Jianjun Zhou,[a] Hui-Hui Cui,[b] Ai-Hua Yuan,*[a] Zhenxing Wang,[c]* Yi-Quan Zhang,*[d] Zhong-Wen Ouyang[c] and You Song*[b]

[a]*School of Environmental and Chemical Engineering, Jiangsu University of Science and Technology, Zhenjiang 212003, P. R. China, E-mail: aihua.yuan@just.edu.cn*

[b]*State Key Laboratory of Coordination Chemistry, Nanjing National Laboratory of Microstructures, School of Chemistry and Chemical Engineering, Nanjing University, Nanjing 210093, P. R. China. E-mail: yousong@nju.edu.cn*

[c]*Wuhan National High Magnetic Field Center & School of Physics, Huazhong University of Science and Technology, Wuhan 430074, P. R. China. E-mail: zxwang@hust.edu.cn*

[d]*Jiangsu Key Laboratory for NSLSCS, School of Physical Science and Technology, Nanjing Normal University, Nanjing 210023, P. R. China. E-mail: zhangyiquan@njnu.edu.cn*

Electronic Supplementary Information

Experimental Section

Materials and Physical measurements

Unless otherwise stated, all chemicals were obtained from commercial sources and used without further purification. $AgBPh_4$ was prepared by metathesis of $NaBPh_4$ and $AgNO_3$ followed by extensive washing with hot distilled H_2O to remove NO_3^- impurities.[S1] Elemental analyses for C, H and N were recorded on an Elementar Vario EL III elemental analyzer. The powder X-ray diffraction (PXRD) patterns for polycrystalline samples were measured at 298 K on a Bruker D8 Advance X-ray Diffratometer. Thermogravimetric (TG) analysis was performed on a thermobalance (STA-499C, NETZSCH). The crystalline sample of **1** was heated from the room temperature to 550 ^oC in N_2 atmosphere. The temperature profile is shown in the following figure:

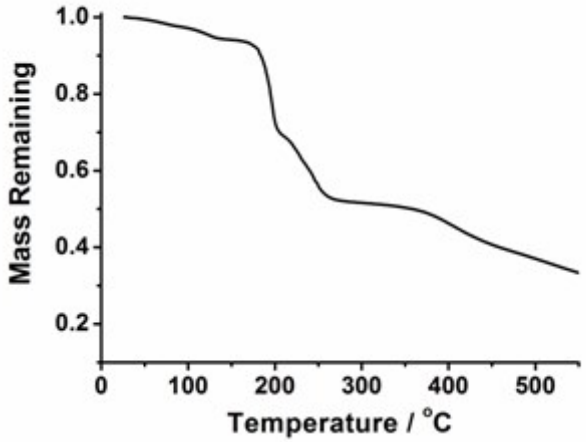

Single-crystal X-ray diffraction data for **1** and **2** were collected on a Bruker APEX II diffractometer at 123 K equipped with a CCD area detector (Mo Kα radiation, λ = 0.71073 Å).[S2–S4] CCDC 1583133 (**1**) and 1583132 (**2**) contain the supplementary crystallographic data for this paper. Direct-current (dc) magnetic measurements of **1** and **2** were performed on a Quantum Design SQUID VSM magnetometer between 2 and 300 K at fields up to 7 T. Alternating-current (ac) susceptibility measurements were carried out at ac frequencies ranging from 1 to 1000 Hz under different applied static fields with an oscillating ac field of 2 Oe. The magnetic susceptibility data were corrected for diamagnetism of the constituent atoms and sample holder estimated by using Pascal constants. HFEPR measurements were performed on a locally developed spectrometer at the Wuhan National High Magnetic Field Center, using a pulsed

magnetic field of up to 30 T.[S5]

Synthesis of $[Co(imidazole)_6][BPh_4]_2 \cdot 0.3CH_3CN$ (**1**)

To a solution of $CoCl_2$ (1.0 mmol, 0.13 g) in 10.0 mL acetonitrile was added a solution of Ag BPh_4 (2.0 mmol, 0.854 g) in 10 mL acetonitrile. The mixture was stirred until the reaction was completed, and then the insoluble silver chloride was removed by filtration. Imidazole (6 mmol, 0.4 mL) was slowly added to the filtrate, and the solution was allowed to stand overnight. The pink block crystals were isolated in 53% yield based on Co content. Elemental analysis (%) calcd for $CoC_{66.6}H_{64.9}B_2N_{12.3}$ (MW 1118.15): C, 71.47; H, 5.80; N, 15.41. Found: C, 71.30; H, 5.87; N,15.30.

Synthesis of $[Co(imidazole)_6][NO_3]_2$ (**2**)

Compound **2** was prepared by the same procedure as what employed for compound **1**, but with using $AgNO_3$ (2.0 mmol, 0.34 g) instead of Ag BPh_4 (2 mmol, 0.854 mL). The red block crystals were isolated in 46% yield based on Co content. Elemental analysis (%) calcd for $CoC_{18}H_{24}N_{14}O_6$ (MW 591.44): C, 36.52; H, 4.06; N, 33.13. Found: C, 36.55; H, 4.00; N, 33.20.

Table S1. Summary of crystal data and refinement for **1** and **2**.

	1	**2**
Molecular formula	$C_{66.6}H_{64.9}B_2CoN_{12.3}$	$C_{18}H_{24}CoN_{14}O_6$
CCDC no	1583133	1583132
Formula weight	1118.15	591.44
Temperature	123(2) K	123(2) K
Wavelength / Å	0.71073	0.71073
crystal system	Monoclinic	Trigonal
Space group	*C2/c*	*R-3*
a / Å	23.170(4)	12.3648(12)
b / Å	13.301(2)	12.3648(12)
c / Å	21.712(3)	14.547(3)
β / deg	118.421(2)	90

V / Å^3	5884.7(16)	1926.1(5)
Z	4	3
D_{calc}, g/cm^3	1.262	1.530
μ / mm^{-1}	0.345	0.732
F (000)	2350	915
Goodness-of-fit on F^2	1.040	1.084
Final R indices [$I > 2\sigma(I)$][a]	R1 = 0.0372, wR2 = 0.0837	R_1 = 0.0235, wR_2 = 0.0597
R indices (all data)[a]	R1 = 0.0488, wR2 = 0.0887	R_1 = 0.0245, wR_2 = 0.0603

[a]$wR_2 = [\Sigma[w(F_o^2-F_c^2)^2]/\Sigma[w(Fo^2)^2]]^{1/2}$, $R_1 = \Sigma||F_o|-|F_c||/\Sigma|F_o|$.

Table S2. Selected Bond Lengths (Å) and Angles (deg) for **1** and **2.**

1				**2**			
Co1-N1	2.1496(13)	N1-Co1-N1a	180.0	Co1-N1	2.1618(10)	N1-Co1-N1d	180.0
Co1-N3	2.1834(13)	N3-Co1-N3a	180.0			N1-Co1-N1a	88.23(4)
Co1-N5	2.1772(13)	N5-Co1-N5a	180.0			N1-Co1-N1b	91.77(4)
		N1-Co1-N3	91.24(5)				
		N1-Co1-N5	90.50(5)				
		N3-Co1-N5	87.79(5)				
		N1-Co1-N3a	88.76(5)				
		N1-Co1-N5a	89.50(5)				
		N3-Co1-N5a	92.21(5)				

Table S3. The fitting results of the EPR and dc magnetic data using the PHI program for **1** and **2**.

		Orbital reduction factor σ	*B0 2* (cm^{-1})	*B2 2* (cm^{-1})
1	EPR	0.96	-43.26	17.37
	Dc magnetic data	1.25	-71.51	13.03
2	EPR	1.36	-63.21	0.93
	Dc magnetic data	1.65	-41.2	4.22

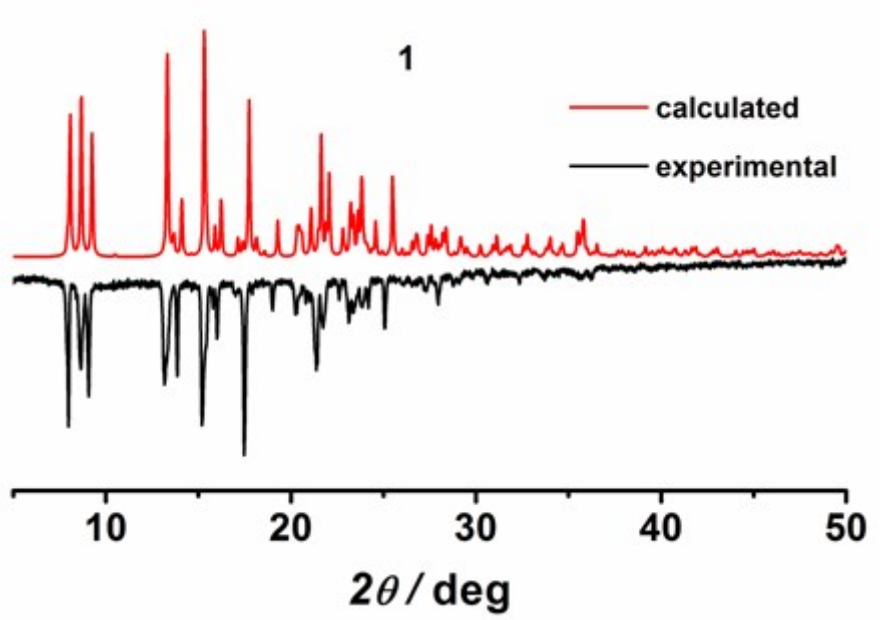

Figure S1. XRD patterns for complexes **1**.

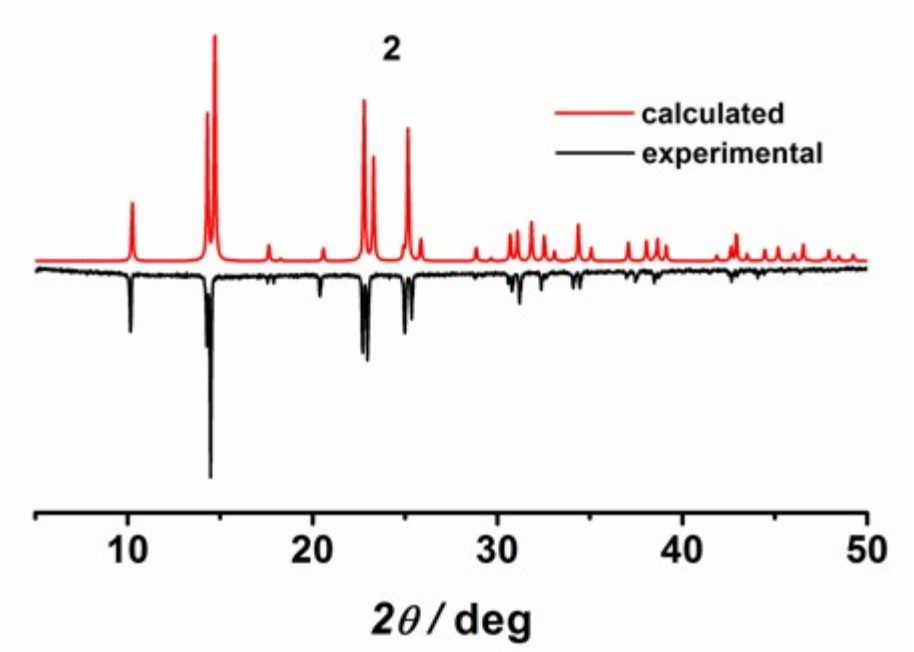

Figure S2. XRD patterns for complexes **2**.

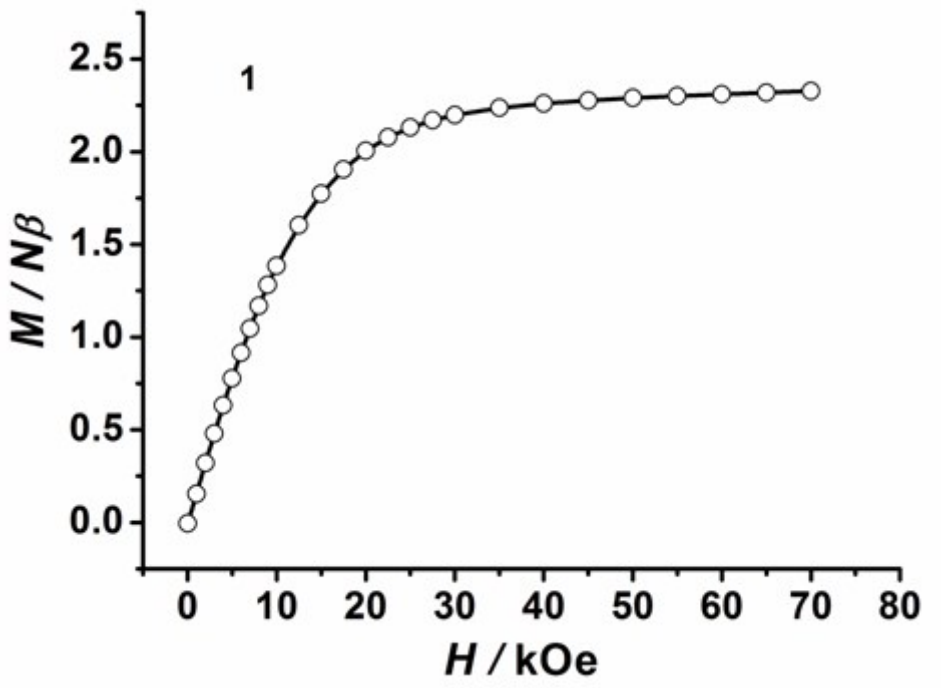

Figure S3. The field-dependence of magnetization at 2 K for **1**. The solid lines are a guide for the eye.

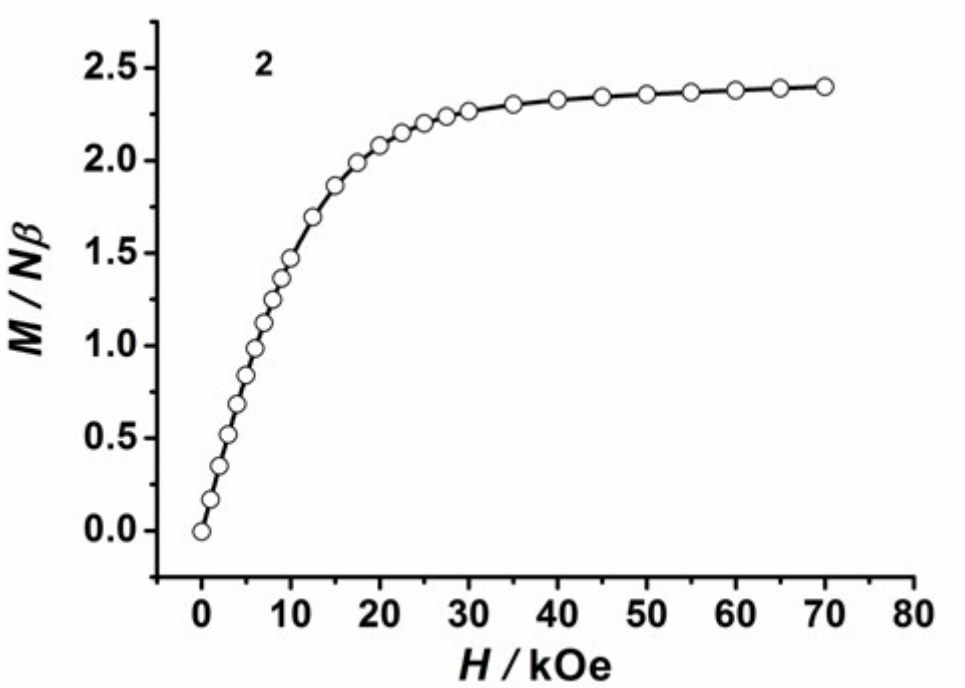

Figure S4. The field-dependence of magnetization at 2 K for **2**. The solid lines are a guide for the eye.

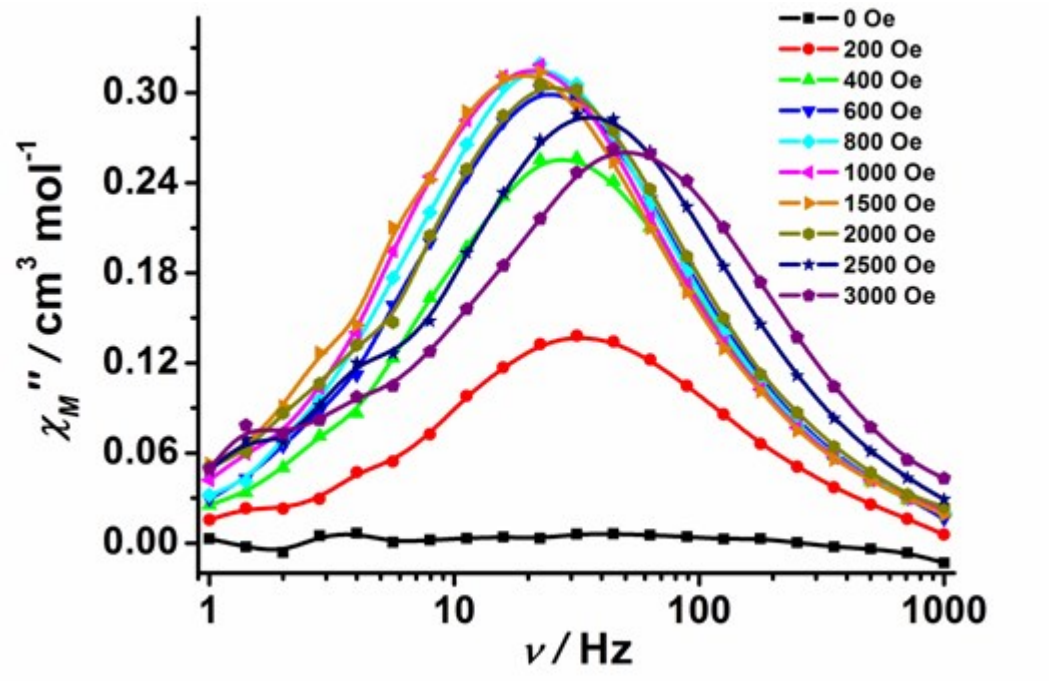

Figure S5. Frequency dependence of out-of-phase (χ_M'') ac susceptibility at 1.8 K under the different applied static fields from 0 to 3000 Oe for **1**. The solid lines are for eye guide.

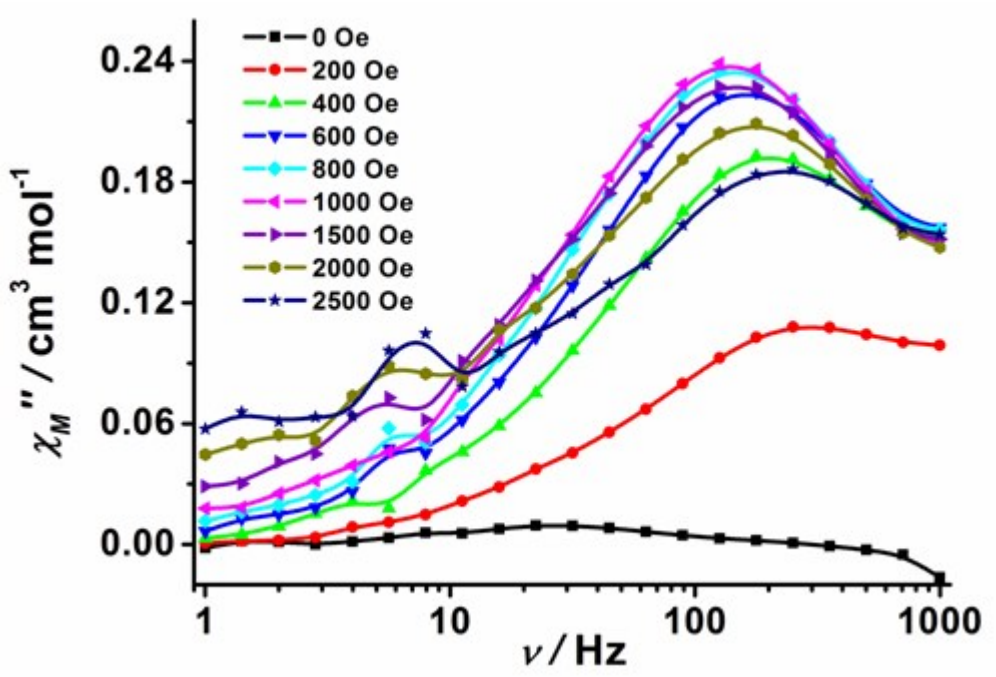

Figure S6. Frequency dependence of out-of-phase (χ_M'') ac susceptibility at 1.8 K under the different applied static fields from 0 to 2500 Oe for **2**. The solid lines are for eye guide.

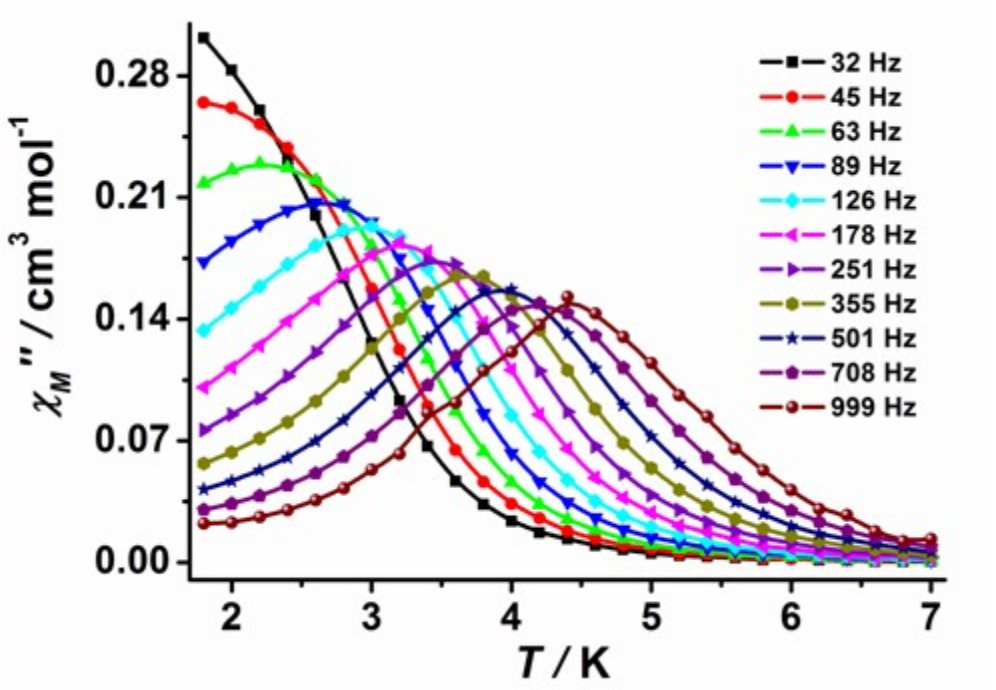

Figure S7. Temperature dependence of out-of-phase ac susceptibility (χ_M'') at different frequency under the dc field of 1000 Oe for **1**. The solid lines are guides for the eye.

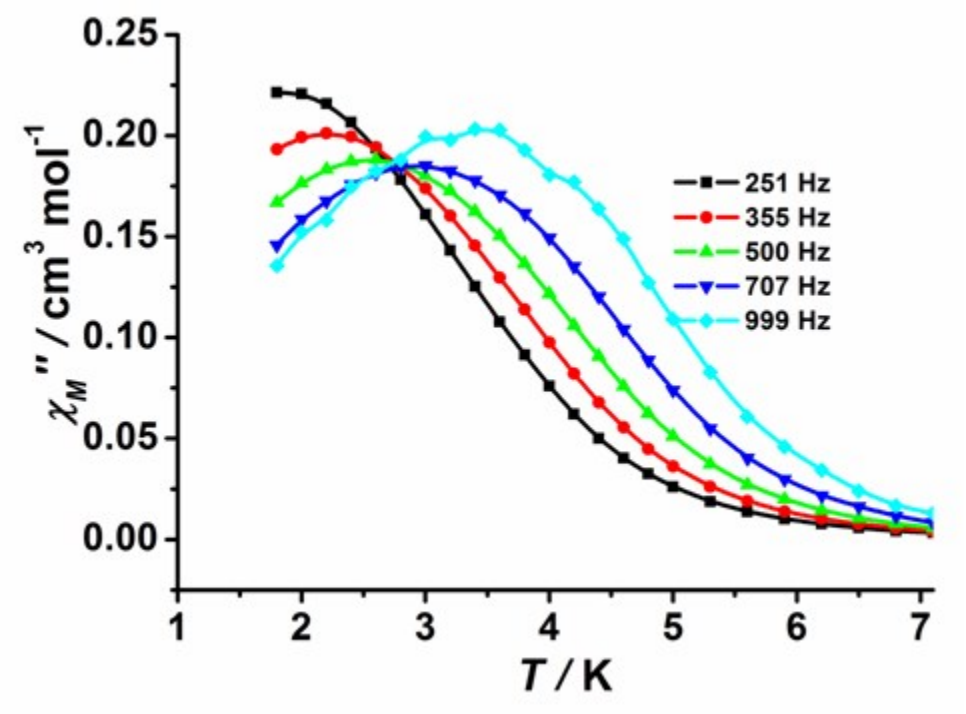

Figure S8. Temperature dependence of out-of-phase ac susceptibility (χ_M'') at different frequency under the dc field of 1000 Oe for **2**. The solid lines are guides for the eye.

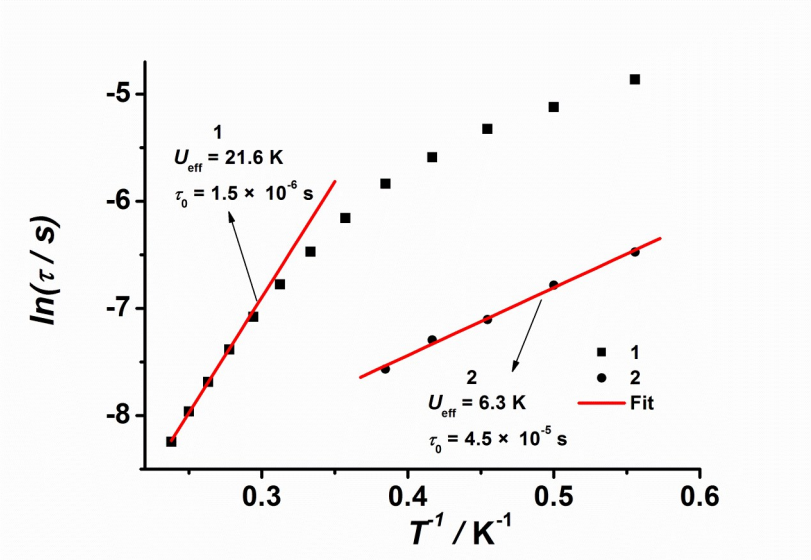

Figure S9. Relaxation time of the magnetization *ln(τ)* vs T^{-1}plots for **1** and **2**. Thesolid lines represent Arrhenius fits.

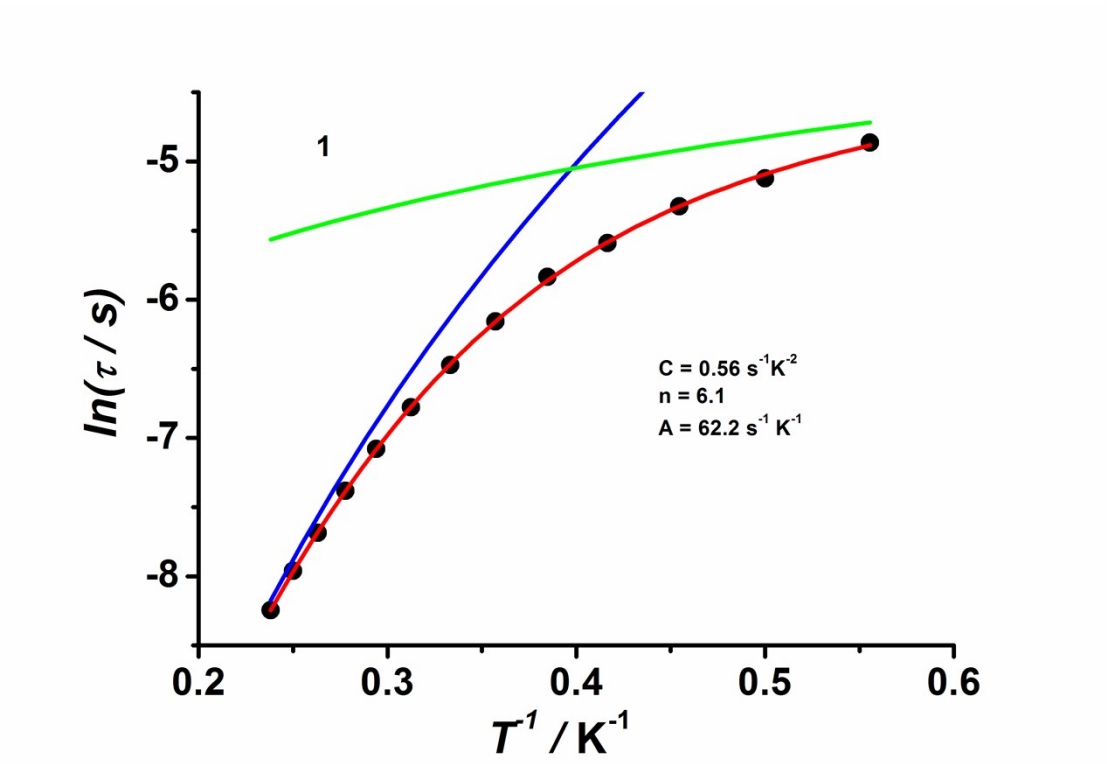

Figure S10. Temperature dependence of the magnetization relaxation rates of **1** under an applied dc field of 1000 Oe. The solid red lines represent the best fit by using a combination of the Raman and direct relaxation mechanisms.

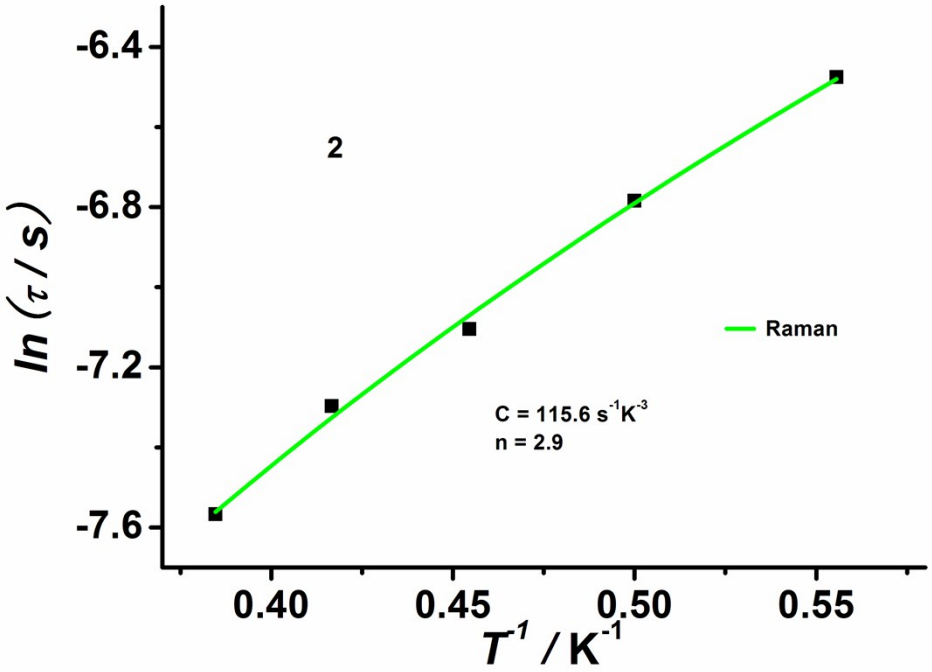

Figure S11. Temperature dependence of the magnetization relaxation rates of **2** under an applied dc field of 1000 Oe. The solid red lines represent the best fit by using a Raman mechanism.

Computational details

Complete active space second-order multiconfigurational perturbation theory (CASPT2) considering the effect of the dynamic electron correlation based on complete-active-space self-consistent field (CASSCF) method with MOLCAS 8.2 program package[S6] was performed on individual Co(II) fragment on the basis of X-ray determined geometry of complexes **1**−**2**. During the calculations, the basis sets for all atoms are atomic natural orbitals from the MOLCAS ANO-RCC library: ANO-RCC-VTZP for Co(II) ion; VTZ for close N; VDZ for distant atoms. The calculations employed the second order Douglas-Kroll-Hess Hamiltonian, where scalar relativistic contractions were taken into account in the basis set. After that, the effect of the dynamical electronic correlation was applied using CASPT2. And then, the spin-orbit couplings were handled separately in the restricted active space state interaction (RASSI-SO) procedure. The active electronsin 10 active spaces considering the 3*d*-double shell effect (5+5′) include all seven 3*d* electrons(CAS(7 in 5+5′)), and the mixed spin-free states are 30 (all from 10 quadrupletsand20 from 40 doublets).

Table S4.Calculated spin-free energies (cm^{-1}) of the lowest ten terms (S = 3/2) of the Co(II) ion of complexes **1**−**2**.

spin-free states	**1**	**2**
	E/cm^{-1}	E/cm^{-1}
1	0.0	0.0
2	79.5	15.0
3	320.7	516.8
4	8342.3	8488.2
5	8494.9	8849.7
6	9462.6	9312.8
7	19135.2	20058.1
8	20648.7	21009.2
9	20927.6	21083.6
10	21204.7	21450.5

Table S5. Calculated weights of the five most important spin-orbit-free states for the lowest two spin-orbit states of the Co(II) ion of complexes **1**−**2**.

	Spin-orbit states	Energy (cm^{-1})	Spin-free states, Spin, Weights				
1	1	0.0	1,1.5,0.4509	2,1.5,0.3475	3,1.5,0.1992	22,0.5,0.0007	4,1.5,0.0004
	2	273.8	1,1.5,0.5898	2,1.5,0.3406	3,1.5,0.0647	4,1.5,0.0013	5,1.5,0.0012
2	1	0.0	1,1.5,0.4422	2,1.5,0.4281	3,1.5,0.1274	22,0.5,0.0006	4,1.5,0.0005
	2	241.9	1,1.5,0.4986	2,1.5,0.4497	3,1.5,0.0462	5,1.5,0.0013	4,1.5,0.0012

Table S6. Calculated energy levels (cm^{-1}), $\boldsymbol{g}$(g_x, g_y, g_z) tensors of the ground and first excited doublets of the Co(II) of complexes **1**−**2**.

	1		**2**	
	E/cm^{-1}	$\boldsymbol{g}$	E/cm^{-1}	$\boldsymbol{g}$
1	0.0	3.373 3.994 5.597	0.0	3.000 3.092 6.555
2	273.8	0.791 1.337 3.041	241.9	2.207 2.004 1.621

Reference

S1 R. F. Jordan and S. F. Echols, *Inorg. Chem.*, 1987, **26**, 383-386.

S2 SMART & SAINT, Software Reference Manuals, version 6.45, Bruker Analytical X-ray Systems, Inc., Madison, WI, 2003.

S3 G. M. Sheldrick, *SADABS – Software for Empirical AbsorptionCorrection*, version 2.05,University of Göttingen, Göttingen, Germany, 2002.

S4 (a) G. M. Sheldrick, *SHELXL97 – Program for Crystal Structure Refinement*, University of Göttingen, Göttingen, Germany, 1997; (b) G. M. Sheldrick, *Acta Cryst.*, 2015, **C71**, 3-8.

S5 (a) S. L. Wang, L. Li, Z. W. Ouyang, Z. C. Xia, N. M. Xia, T. Peng and K. B. Zhang, *Acta Phys. Sin.*, 2012, **61**, 107601; (b) H. Nojiri and Z. W. Ouyang, *Terahertz Sci. Technol.*, 2012, **5**, 1.

S6 Karlström, G.; Lindh, R.; Malmqvist, P.-Å.; Roos, B. O.; Ryde, U.; Veryazov, V.; Widmark, P.-O.; Cossi, M.; Schimmelpfennig, B.; Neograd y, P.; Seijo, L. MOLCAS: a Program Package for Computational Chemistry. *Comput. Mater. Sci*., 2003, **28**, 222.